Article

Cell Reports

# Presenilin 1 Maintains Lysosomal $Ca^{2+}$ Homeostasis via TRPML1 by Regulating vATPase-Mediated Lysosome Acidification

## Graphical Abstract

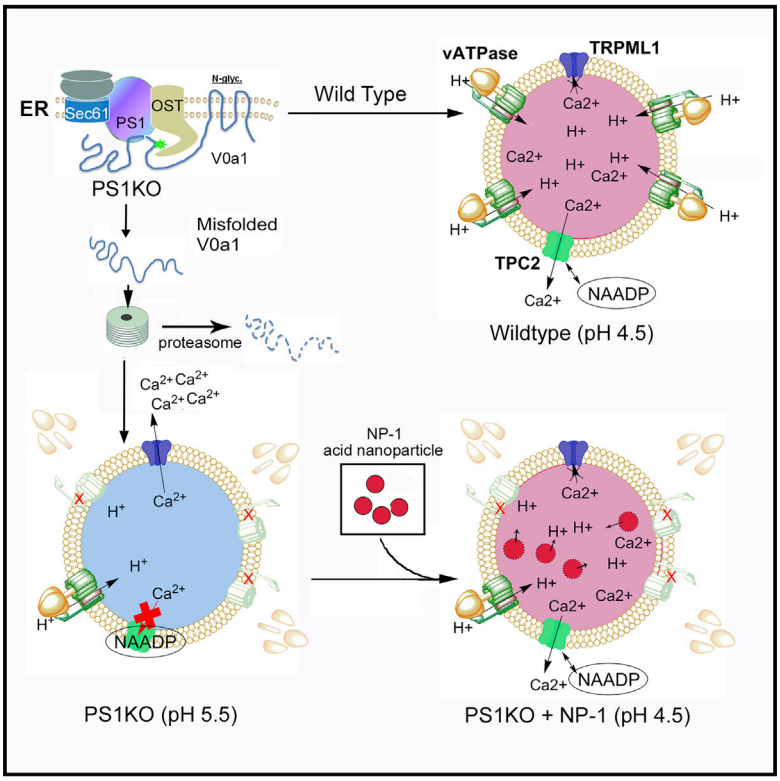


## Highlights

- PS1 is essential for V0a1 subunit glycosylation, stability, and vATPase assembly
- PS1 deficiency depletes vATPase, impairing lysosomal acidification and proteolysis
- Defective lysosome acidification in PS1KO cells causes lysosomal $Ca^{2+}$ efflux
- TRPML1 mediates lysosomal $Ca^{2+}$ efflux and cytosolic $Ca^{2+}$ elevation in PS1KO cells

## Authors

Ju-Hyun Lee, Mary Kate McBrayer, Devin M. Wolfe, ..., Claire H. Mitchell, Emyr Lloyd-Evans, Ralph A. Nixon

## Correspondence

nixon@nki.rfmh.org

## In Brief

Lee et al. present evidence establishing that Presenilin 1 loss of function elevates lysosomal pH via loss of V0a1 vATPase subunits. Besides disrupting autophagy, elevated lysosomal pH hyperactivates the TRPML1 calcium channel, causing increased lysosomal calcium efflux and cytosolic calcium elevation, thus linking two AD-related presenilin phenotypes to vATPase deficiency.

Lee et al., 2015, Cell Reports *12*, 1430–1444
September 1, 2015 
http://dx.doi.org/10.1016/j.celrep.2015.07.050

OPEN ACCESS
CellPress

Cell Reports
Article

# Presenilin 1 Maintains Lysosomal $Ca^{2+}$ Homeostasis via TRPML1 by Regulating vATPase-Mediated Lysosome Acidification

Ju-Hyun Lee,[1,2,9] Mary Kate McBrayer,[1,9] Devin M. Wolfe,[1,9] Luke J. Haslett,[5] Asok Kumar,[1,3] Yutaka Sato,[1] Pearl P.Y. Lie,[1] Panaiyur Mohan,[1,2] Erin E. Coffey,[6] Uday Kompella,[8] Claire H. Mitchell,[6,7] Emyr Lloyd-Evans,[5] and Ralph A. Nixon[1,2,4,*]
[1]Center for Dementia Research, Nathan S. Kline Institute, Orangeburg, NY 10962, USA
[2]Department of Psychiatry
[3]Department of Pathology
[4]Department of Cell Biology
New York University, New York, NY 10016, USA
[5]Division of Pathophysiology and Repair, Cardiff University, Cardiff CF10 3XQ, UK
[6]Department of Anatomy and Cell Biology
[7]Department of Physiology
University of Pennsylvania, Philadelphia, PA 19104, USA
[8]Pharmaceutical Science and Ophthalmology, University of Colorado, Aurora, CO 80045, USA
[9]Co-first author
*Correspondence: nixon@nki.rfmh.org
http://dx.doi.org/10.1016/j.celrep.2015.07.050


## SUMMARY

**Presenilin 1 (PS1) deletion or Alzheimer's disease (AD)-linked mutations disrupt lysosomal acidification and proteolysis, which inhibits autophagy. Here, we establish that this phenotype stems from impaired glycosylation and instability of vATPase V0a1 subunit, causing deficient lysosomal vATPase assembly and function. We further demonstrate that elevated lysosomal pH in Presenilin 1 knockout (PS1KO) cells induces abnormal $Ca^{2+}$ efflux from lysosomes mediated by TRPML1 and elevates cytosolic $Ca^{2+}$. In WT cells, blocking vATPase activity or knockdown of either PS1 or the V0a1 subunit of vATPase reproduces all of these abnormalities. Normalizing lysosomal pH in PS1KO cells using acidic nanoparticles restores normal lysosomal proteolysis, autophagy, and $Ca^{2+}$ homeostasis, but correcting lysosomal $Ca^{2+}$ deficits alone neither re-acidifies lysosomes nor reverses proteolytic and autophagic deficits. Our results indicate that vATPase deficiency in PS1 loss-of-function states causes lysosomal/autophagy deficits and contributes to abnormal cellular $Ca^{2+}$ homeostasis, thus linking two AD-related pathogenic processes through a common molecular mechanism.**

## INTRODUCTION

Presenilin 1 (PS1) is primarily known to be a catalytic component of γ-secretase complex, which carries out cleavage of amyloid precursor protein yielding Abeta peptides, which in various forms have been implicated in AD pathogenesis (Chávez-Gutiérrez et al., 2012; De Strooper and Annaert, 2010; Selkoe and Wolfe, 2007; Steiner and Haass, 2000). Loss-of-function mutations of PS1 that cause early-onset Alzheimer's disease (AD) alter the proportion of Abeta 42 and 40 peptides (Chávez-Gutiérrez et al., 2012), which is considered critical to their neurotoxicity and a major contributor to AD pathogenesis. Increasing evidence, however, indicates that PS1 serves additional γ-secretase-independent roles in wnt signaling (Kang et al., 1999), endoplastmic reticulum (ER) $Ca^{2+}$ regulation (Shilling et al., 2014; Tu et al., 2006), as well as lysosomal function and autophagy (Coen et al., 2012; Lee et al., 2010; Wilson et al., 2004; Wolfe et al., 2013). PS1 dysfunction is therefore likely to contribute in multiple ways to AD pathogenesis by altering Abeta clearance, production, and oligomerization (Nixon, 2007) and corrupting diverse lysosomal functions via the massive buildup of incompletely degraded autophagic substrates in lysosomes, a characteristic feature of the neuritic dystrophy in AD (Nixon and Yang, 2012). Lysosomal dysfunction in neurons is closely tied to neurodegeneration and cell death mechanisms (Česen et al., 2012; Nixon and Yang, 2012). Growing genetic and biochemical evidence implicates dysfunction of the endosomal-lysosomal and autophagic lysosomal pathways in the pathogenesis of a number of neurodegenerative disorders, including AD, Parkinson's disease, and amyotrophic lateral sclerosis (ALS) (Frakes et al., 2014; Ghavami et al., 2014; Menzies et al., 2015; Nixon, 2013). The therapeutic efficacy of autophagy/lysosome modulation in animal models of these disorders (Butler et al., 2011; Sun et al., 2008; Yang et al., 2011) further underscores the significance of lysosomal impairments to disease pathogenesis.

It has been shown that loss of PS1 function in multiple cell types disrupts lysosome acidification, leading to markedly impaired autophagy (Avrahami et al., 2013; Dobrowolski et al., 2012; Lee et al., 2010; Torres et al., 2012; Wolfe et al., 2013).

Controversial reports from two groups (Coen et al., 2012; Zhang et al., 2012a), however, proposed that PS1 plays no role in lysosomal pH, lysosomal proteolysis, or vATPase subunit maturation and that the V0a1 subunit specifically implicated in our studies is not involved in lysosomal acidification.

Here, we directly demonstrate deficiencies in lysosomal vATPase content and function in lysosomes of Presenilin 1 knockout (PS1KO) cells and establish the role of failed vATPase V0a1 subunit maturation in PS1-dependent lysosomal acidification failure, leading to defective autophagy and abnormal efflux of lysosomal $Ca^{2+}$. We further show that the secondary abnormalities in lysosomal $Ca^{2+}$ efflux are caused by a pH-modulated activation of the low $H^{+}$-sensitive endolysosomal $Ca^{2+}$ channel, transient receptor potential cation channel mucolipin subfamily member 1 (TRPML1) (Raychowdhury et al., 2004), and are responsible for substantial elevations of cytosolic $Ca^{2+}$ in PS1-deficient cells. We present further evidence that the V0a1 subunit is essential for lysosome acidification in neurons and non-neural cells and that inhibiting vATPase function in WT cells recapitulates the PS1KO phenotype. Restoring normal lysosomal pH using lysosome-targeted acidic nanoparticles reverses these abnormalities, but the correction of lysosomal $Ca^{2+}$ deficits alone does not, thus implying that lysosomal pH modulates TRPML1 activation and $Ca^{2+}$ efflux as a secondary consequence of vATPase deficiency in PS1KO cells. Our studies, therefore, link two $\gamma$-secretase-independent effects of PS1, each having pathogenic significance in AD, and demonstrate that vATPase deficiency is a common underlying mechanism.

## RESULTS

### PS1-Dependent Regulation of Lysosomal pH Is Essential for Lysosomal $Ca^{2+}$ Homeostasis Mediated by TRPML1

To investigate the relationship between defects in lysosomal $Ca^{2+}$ homeostasis and lysosomal acidification in PS1KO cells, we measured lysosomal $Ca^{2+}$ levels and observed lowered lysosomal $Ca^{2+}$ levels, as previously reported (Coen et al., 2012) and concomitantly elevated cytosolic $Ca^{2+}$ levels (Figure 1A). We confirmed lysosomal $Ca^{2+}$ reduction by assaying $Ca^{2+}$ release after pretreatment with ionomycin to release all internal, non-lysosomal calcium stores (Lloyd-Evans et al., 2008), followed by glycyl-L-phenylalanine-beta-naphthylamide (GPN) to induce lysosomal rupture causing the release of lysosomal $Ca^{2+}$ (Penny et al., 2014). Interestingly, GPN elevated cytosolic $Ca^{2+}$ due to lysosomal $Ca^{2+}$ release after ionomycin treatment in WT, but had minimal effect on PS1KO cells (Figure 1B). To confirm in PS1KO cells that reduced lysosomal $Ca^{2+}$ release after GPN is due to deficient lysosomal calcium stores, we treated WT cells with U18666a, a control agent used to deplete lysosomal $Ca^{2+}$ stores without affecting vATPase function (Lloyd-Evans et al., 2008). As expected, U18666A-treated WT cells exhibited a marked reduction in the rise of cytosolic $Ca^{2+}$ due to lysosomal $Ca^{2+}$ release following addition of ionomycin and then GPN. Importantly, the magnitude of the reduction of lysosomal $Ca^{2+}$ release was similar to that observed in untreated PS1KO cells (Figure 1B), again showing that levels of lysosomal $Ca^{2+}$ are markedly lowered in PS1KO cells.

Lysosomal $Ca^{2+}$ channels, including TPC1/2, are NAADP dependent and sensitive to lysosomal pH. At normal lysosomal pH, elevated cytosolic NAADP transiently binds the channel, triggering lysosomal $Ca^{2+}$ release, but at elevated lysosomal pH, TPC2 channels are blocked because NAADP cannot dissociate to re-trigger additional $Ca^{2+}$ release (Pitt et al., 2010). We investigated the effects of NAADP-AM after clamping the ER store with thapsigargin. Untreated WT cells showed an increase in cytosolic $Ca^{2+}$ after NAADP-AM addition (Figure 1C), and pretreatment with U18666A reduced the rise in cytosolic $Ca^{2+}$, reflecting the loss of $Ca^{2+}$ from the lysosome (Figures 1B and 1C). By contrast, PS1KO cells showed no NAADP-dependent $Ca^{2+}$ release (Figure 1C) despite the presence of a remaining, albeit diminished, lysosomal $Ca^{2+}$ pool (Figures 1A and 1B). Given that elevated lysosomal pH blocks TPC channels, the lack of response to NAADP-AM in PS1KO cells provided further evidence for a lysosomal pH defect and implied a different cause for $Ca^{2+}$ leak. Because of a lack of NAADP-mediated lysosomal $Ca^{2+}$ release in PS1KO cells, we investigated the cause of the reduced lysosomal $Ca^{2+}$ levels by focusing on another endolysosomal $Ca^{2+}$ permeant channel reported to be activated in its endogenous state by elevated lysosomal pH, namely TRPML1 (Raychowdhury et al., 2004).

To analyze the lysosomal pH dependence of TRPML1 activity in PS1KO cells, we first altered lysosomal proton content with $NH^{4+}$, which alkalinizes the lysosome only at high concentrations, thereby inducing $Ca^{2+}$ leak and emptying lysosomal $Ca^{2+}$ stores (Christensen et al., 2002). We hypothesized that a weak lysosomal alkalinization stimulus (5 mM, <2 min), which does not affect lysosomal pH in WT cells (data not shown), would trigger $Ca^{2+}$ leak more readily in the elevated lysosomal pH in PS1KO cells. As expected, this condition triggered a significant $Ca^{2+}$ leak from PS1KO compared to WT cells (Figure 1D). These data indicated that PS1KO cells more readily leak $Ca^{2+}$ with the addition of small amounts of an alkalinizing agent and suggested that other pH sensitive channels, like TRPML1, might become hyperactive at elevated pH. To investigate this hypothesis, we treated cells with the TRPML1 agonist ML-SA1 (Grimm et al., 2010). Although a low dose (20 $\mu$M) of ML-SA1 induced only a minimal elevation in cytosolic $Ca^{2+}$ in WT cells (Figure 1E), cytosolic $Ca^{2+}$ rose markedly in PS1KO cells (Figure 1E).

While TPC2 and TRPML1 are functionally distinct (Yamaguchi et al., 2011), they are both activated by phosphoinositols (Dong et al., 2010; Jha et al., 2014), suggesting that they could both be inhibited by similar ligands. Ned-19, an NAADP analog, inhibits activation of NAADP-dependent lysosomal $Ca^{2+}$ channels preventing $Ca^{2+}$ efflux (Naylor et al., 2009). Surprisingly, Ned-19 pretreatment of PS1KO cells inhibited TRPML1, and cytosolic $Ca^{2+}$ elevation induced by ML-SA1 was now corrected back to WT levels in the Ned-19-treated PS1KO cells (Figure 1E).

Given that Ned-19 has been previously known to inhibit only lysosomal NAADP-dependent $Ca^{2+}$ channels, we investigated the possibility that Ned-19 inhibits channels in addition to TPC2 by knocking down TPC2 in PS1KO cells. Knockdown of TPC2 had no effect on either lysosomal or cytosolic $Ca^{2+}$ levels (Figures 1F and S1A), confirming that it is inactive at the abnormally high lysosomal pH. However, consistent with the idea that Ned-19 can target other lysosomal $Ca^{2+}$ channels, Ned-19 increased

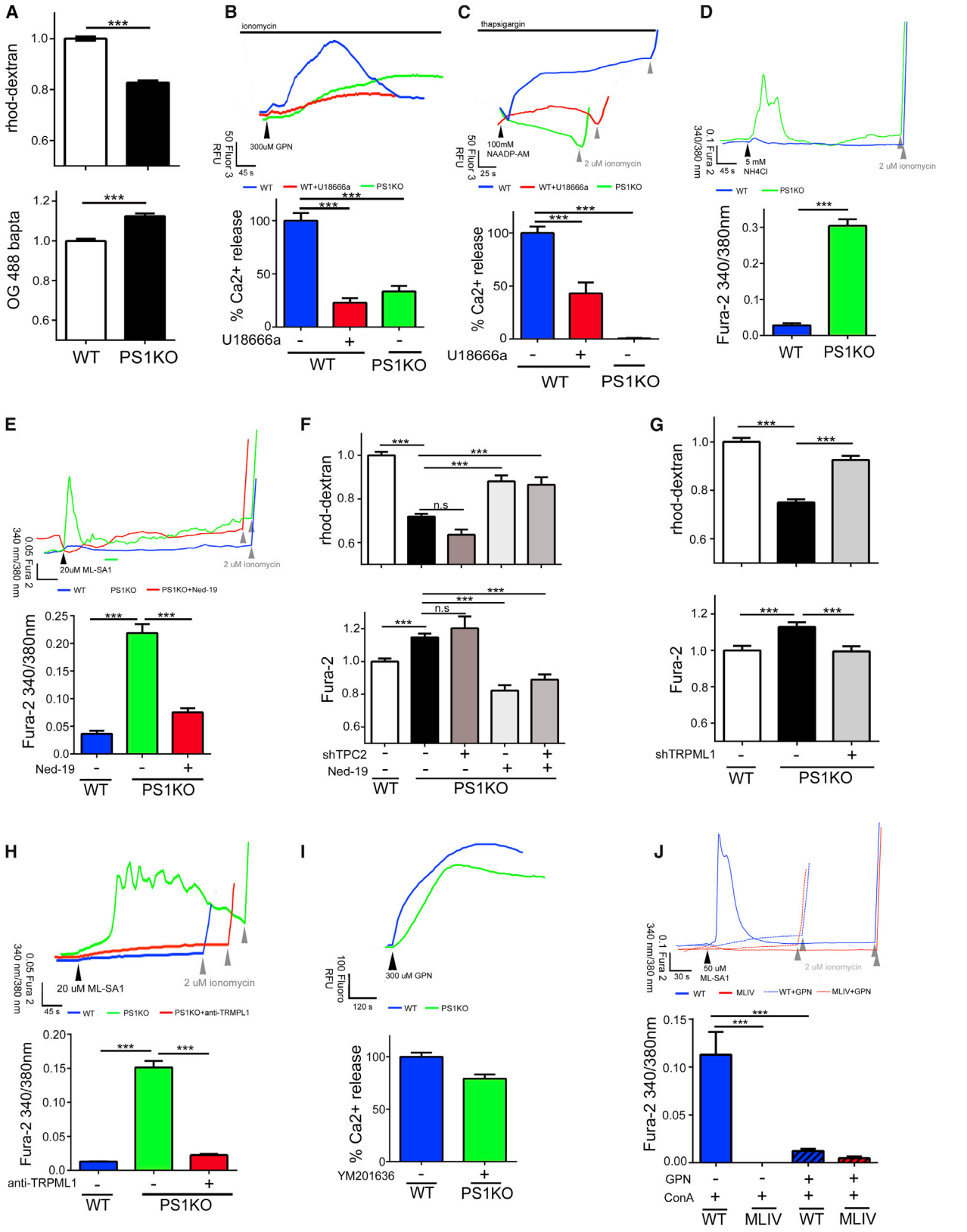


*(legend on next page)*

lysosomal $Ca^{2+}$ and decreased cytosolic $Ca^{2+}$ in both PS1KO and shTPC2 PS1KO cells (Figure 1F). To verify that TRPML1 is the primary $Ca^{2+}$ efflux channel in PS1KO cells, we knocked down TRPML1 in PS1KO cells, which restored both lysosomal and cytosolic $Ca^{2+}$ to near WT levels (Figures 1G and S1A). Moreover, an anti-TRPML1 antibody that inhibited the activation of the channel (Zhang et al., 2009) efficiently inhibited the rise in cytosolic $Ca^{2+}$ induced by ML-SA1 (Figure 1H). As additional confirmation, we treated PS1KO cells with YM201636 to inhibit the synthesis of PI(3,5)P2, the endogenous potentiator of TRPML1 channel opening (Zhang et al., 2012b), which reduced the opening frequency of TRPML1. After GPN-induced rupture of lysosomal membranes, cytosolic $Ca^{2+}$ rose in PS1KO cells to levels nearly equal to those of WT cells, indicating an increase in the releasable pool of lysosomal $Ca^{2+}$ (Figure 1I).

We confirmed that TRPML1 is responsible for depleting lysosomal $Ca^{2+}$ at the elevated pH in PS1KO cells by demonstrating that concanamycin A (ConA) inhibition of vATPase activity in control human fibroblasts induced a PS1KO-like elevation of lysosomal $Ca^{2+}$ release in response to the TRPML1 agonist ML-SA1, whereas MLIV human fibroblasts, containing inactive TRPML1, showed no response (Figure 1J), indicating an elevation of lysosomal pH can induce hyperactivation of TRPML1. The rise in cytosolic $Ca^{2+}$ under ML-SA1 conditions originated at the lysosome and via TRPML1 because cytosolic $Ca^{2+}$ in control and MLIV human fibroblasts pretreated with GPN did not rise after additional treatment with ML-SA1 (Figure 1J).

Collectively, these data indicate that the presence of an elevated $Ca^{2+}$ leak out of PS1KO lysosomes is mediated by TRPML1, which is hyperactivated in PS1KO cells due to elevated lysosomal pH.

## Restoring Normal Lysosomal pH, but Not Lysosomal $Ca^{2+}$ Homeostasis Alone, Rescues Lysosomal Deficits and Autophagy

Lysosomal $Ca^{2+}$ dysfunction caused by PS1 deletion was proposed to be responsible for autophagy deficits in PS1KO cells (Coen et al., 2012), although no evidence or underlying mechanism was shown. Because treatment of PS1KO cells with Ned-19 normalized TRPML1 activity (Figure 1E) and prevented abnormal lysosomal $Ca^{2+}$ efflux, we investigated whether or not reducing this $Ca^{2+}$ leak influences lysosomal pH or lysosome-related function. Although Ned-19 treatment of PS1KO cells restored normal lysosomal and cytosolic $Ca^{2+}$ levels (Figure 2A), its addition to PS1KO cells had no ameliorative effects on lysosomal pH (Figure 2B), levels of LC3-II (Figure 2C), or CatD activation in lysosomes measured using Bodipy FL-pepstatin A (Figure 2D).

Cells were transiently transfected with the eGFP-mRFP-LC3 construct and treated with Ned-19 to assess any alterations in autophagic flux. Compared with WT controls, untreated PS1KO cells display a lower percentage of red puncta and an elevated percentage of yellow puncta, indicating defective maturation of autophagosomes into acidic lysosomes. Ned-19 did not affect these percentages, indicating that lysosomal $Ca^{2+}$ restoration did not restore lysosomal acidity or autophagic flux (Figure 2E). EM morphometry confirmed these results by showing that Ned-19 did not alter the abnormally lowered ratio of lysosomes to late AVs in PS1KO cells (Figure S2A). Previously, we demonstrated that autophagy induction was not altered in PS1KO cells and that reduced autophagic flux was due specifically to delayed lysosomal degradation (Lee et al., 2010). Establishing that Ned-19 does not influence autophagy induction, we observed that Ned-19 treatment does not alter levels of either p-mTOR or p-P70S6K in PS1KO cells (Figure S2B). Thus, the key driver of autophagic dysfunction in PS1KO cells, namely markedly delayed degradation, is not due to $Ca^{2+}$ dysfunction, as previously speculated (Coen et al., 2012).

Contrasting with the minimal effect of lysosomal $Ca^{2+}$ correction on autophagy, reversal of lysosomal pH deficits in PS1KO cells rapidly normalized autophagy and lysosomal function, including $Ca^{2+}$ efflux. We were able to lower intraluminal lysosomal pH using a poly (DL-lactide-co-glycolide) (PLGA) acidic nanoparticle, which is internalized in cells by endocytosis and targeted to lysosomes where protons are released in the lysosomal lumen through hydrolysis of poly-lactic acid (Baltazar et al., 2012). We identified a nanoparticle species, designated NP-1, as having optimal uptake efficiency and ability to restore lysosomal pH as previously shown in ARPE-19 cells (Baltazar et al., 2012). Exposure of PS1KO cells to NP-1 normalized lysosomal pH, lowering it from 5.7 to 4.6 (Figure 2F). Pretreatment with NP-1 for 24 hr normalized TRPML1 activity, as no rise in cytosolic $Ca^{2+}$ was elicited with ML-SA1

**Figure 1. TRMPL1 Mediates Lysosomal $Ca^{2+}$ Efflux in PS1KO Cells**

(A) Lysosomal $Ca^{2+}$ is reduced (WT, n = 336; PS1KO, n = 338), and cytosolic $Ca^{2+}$ is elevated in PS1KO cells (WT, n = 148; PS1KO, n = 150).

(B) Cells were treated with 5 μM ionomycin followed by GPN (300 μM) to measure lysosomal $Ca^{2+}$ levels. Less $Ca^{2+}$ is released from PS1KO (n = 18) cells. WT cells treated for 24 hr with 2 μg/ml U18666a (n = 33) release less lysosomal $Ca^{2+}$.

(C) Compared to WT (n = 67), PS1KO cells (n = 93) released minimal $Ca^{2+}$ after 1 μM thapsigargin followed by NAADP-AM (100 nM) (arrowhead). $Ca^{2+}$ release was significantly lowered in WT cells treated with U18666a (n = 25).

(D) Addition of 5 mM $NH_4Cl$ increased cytosolic $Ca^{2+}$ in PS1KO (n = 64) but not WT cells (n = 125).

(E) Twenty μM ML-SA1 (black arrowhead) elevated cytosolic $Ca^{2+}$ levels in PS1KO (n = 151) but not WT cells (n = 206), and this elevation was diminished by Ned-19 (0.5 μM, 24 hr, n = 167) (gray arrowheads indicate ionomycin addition).

(F) Seventy-two hr shRNA TPC2KD had no discernible effect on lysosomal or cytosolic $Ca^{2+}$ levels in PS1KO cells (n > 90); 0.5 μM Ned-19 (24 hr) restored lysosomal and cytosolic $Ca^{2+}$ levels even when TPC2 was knocked down.

(G) Seventy-two hr knockdown of TRPML1 significantly elevated lysosomal $Ca^{2+}$ and decreased cytosolic $Ca^{2+}$ in PS1KO cells.

(H) Anti-TRMPL1 antibody (16 hr, 5 μg/ml) inhibited ML-SA1-mediated lysosomal $Ca^{2+}$ release in PS1KO cells (n = 60).

(I) Lysosomal $Ca^{2+}$ levels determined using GPN are almost normalized in PS1KO cells after 10 μM YM201636 for 1 hr via reduced $Ca^{2+}$ flux through TRPML1 (n = 100).

(J) ConA followed by ML-SA1 induced a rise in cytosolic $Ca^{2+}$ in WT (n = 33) but not MLIV fibroblasts (n = 29) imaged in a $Ca^{2+}$-free buffer. Osmotic lysis of lysosomes with GPN prior to ML-SA1 abolished $Ca^{2+}$ release in WT (n = 11) and MLIV cells (n = 17). ***$p < 0.0001$. Error bars are ± SEM.

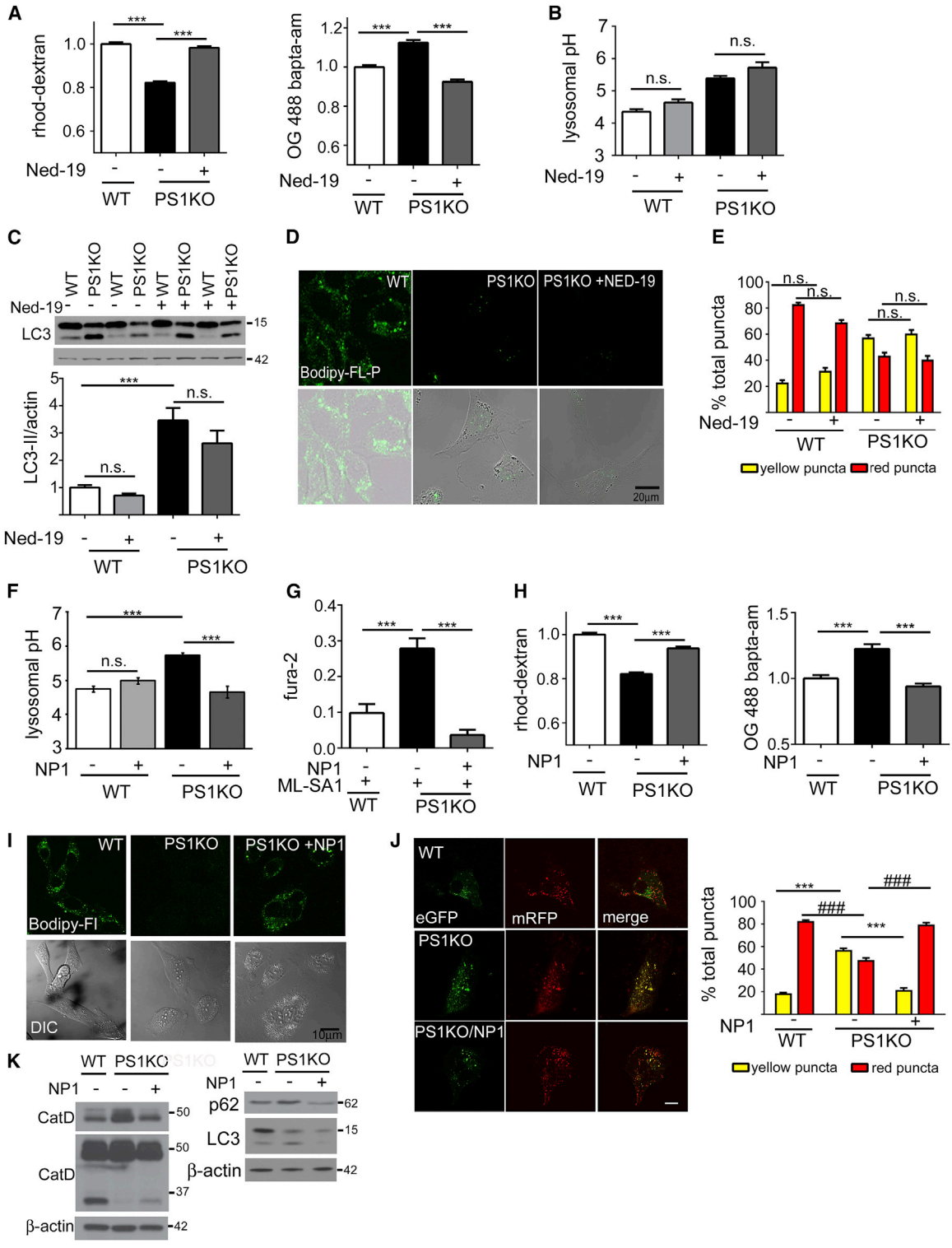


**Figure 2. Restoring Normal Lysosomal pH, but Not Lysosomal $Ca^{2+}$ Homeostasis Alone, Rescues Lysosomal Deficits and Autophagy**

(A) Ned-19 (0.5 μM, 24 hr) elevated lysosomal $Ca^{2+}$ (WT n = 453; PS1KO n = 461; PS1KO/Ned-19 n = 522) and decreased cytosolic $Ca^{2+}$ levels in PS1KO cells (WT n = 148; PS1KO n = 150; PS1KO/Ned-19 n = 150).

(B) Ned-19 does not alter lysosomal pH in WT or PS1KO cells (n = 9 each).

(C and D) Ned-19 does not reduce elevated LC3-II levels in PS1KO cells (C) (n = 11) or increase in situ CatD activity (D) (n = 3). Scale bars represent 20 μm.

*(legend continued on next page)*

(Figure 2G), similar to the lack of effect of ML-SA1 on WT cells (Figure 1E). The normalization of lysosomal $Ca^{2+}$ and decrease in cytosolic $Ca^{2+}$ levels support the hypothesis that lysosomal $Ca^{2+}$ levels are dependent on lysosomal acidification (Figure 2H). In addition, we observed that lysosomal pH correction with NP-1 fully restored CatB and CatD activities in PS1KO lysosomes in situ measured with MR-CatB and Bodipy-pepstatin A, respectively (Figures 2I and S2C), as well as levels of mature CatD. Accumulation of the autophagy substrates, p62 and LC3-II, were also markedly decreased (Figure 2K). Moreover, NP-1 decreased the percentage of yellow eGFF-mRFP-LC3 puncta by 50% and increased the percentage of red puncta by ~30% in PS1KO cells, reflecting a restoration of autophagic flux at the lysosomal clearance stage of autophagy (Figure 2J) given that autophagy induction markers p-mTOR and p-p70S6K were unaltered by NP-1 (Figure S2D). Furthermore, V0a1 glycosylation was unchanged by NP-1, indicating that reacidification was due to protein release from the nanoparticle and not to amelioration of vATPase deficits (Figure S2E).

### Elevated Lysosomal $Ca^{2+}$ Efflux in PS1KO Cells Is Secondary to Defective Lysosomal Acidification and Can Be Induced in WT Cells by vATPase Inhibition

Treatment of WT cells with the vATPase inhibitor, ConA, elevated lysosomal pH to a level similar to that in untreated PS1KO cells (Figure 3A) and did not further elevate lysosomal pH in PS1KO cells (Figure 3A). These results are consistent with previous evidence that, despite a high level of vATPase inhibition, cells can still achieve a moderate degree of lysosomal acidification (Mindell, 2012). Supporting the close relationship between pH and $Ca^{2+}$ content in lysosomes, ConA decreased lysosomal $Ca^{2+}$ and elevated cytosolic $Ca^{2+}$ in WT cells (Figure 3B) but, as expected, did not alter the already abnormal levels of lysosomal and cytosolic $Ca^{2+}$ in PS1KO cells where vATPase function is substantially compromised (Figure 3B). Importantly, ConA inhibition of vATPase activity in WT cells reproduced previously reported PS1KO lysosome and autophagy deficits, including elevated LC3-II levels (Figure 3C), lowered CatD activity (Figure 3D), lowered CatB activity (Figure 3E), increased late AV accumulation, and decreased lysosome number (Figure 3F) and autophagic flux measured using the tandem EGFP-mRFP LC3 reporter (Figure 3G). Moreover, ConA treatment had no effect on autophagic induction, as both p-mTOR and p-p70S6K levels remained unchanged (Figure S2F).

### PS1 Deletion Leads to Loss of Lysosomal vATPase Activity

We previously reported reduced V0a1 subunit maturation and levels in PS1KO cells (Lee et al., 2010; Wolfe et al., 2013). To investigate this issue further specifically in lysosomes, we used a superparamagnetic chromatography isolation procedure (Walker and Lloyd-Evans, 2015) to isolate highly enriched lysosomal preparations from PS1KO and WT cells, comprising 3% of the total cell lysate (protein: protein) and representing an enrichment of the LAMP2 lysosomal marker. Western blot analysis of enriched lysosomes confirmed the purity of lysosome fractions by demonstrating the presence of minimal calnexin and EEA1 and strong enrichment of LC3-II and CatD (Figure 4A). The mature active form of CatD was diminished in PS1KO lysosomes, as previously seen in intact cells (Lee et al., 2010). The V0a1 subunit in purified lysosomes from PS1KO cells was present at markedly lowered levels compared to those in WT lysosomes and existed predominantly at a lower apparent molecular weight in PS1KO lysosomes, consistent with it being incompletely glycosylated, as previously reported (Lee et al., 2010). The ratio of V0a1 relative to LAMP2 used as a lysosome loading control was lowered 70% in PS1KO lysosomes (Figure 4B). We next analyzed the assembly of the vATPase complex on isolated lysosomes by measuring levels of lysosomal V1E1 subunit, which actively assembles with the membrane bound V0 subcomplex during formation of the complete vATPase. V1E1 on PS1KO lysosomes was reduced to similar levels as V0a1 (Figure 4B), substantiating earlier findings on crude membrane fractions from PS1KO cells (Lee et al., 2010).

To assess activity of the assembled vATPase in purified lysosomes, we next measured the ATP-hydrolytic activity of the complex and its proton pumping capacity directly. The ATP hydrolysis rate, monitored by release of inorganic phosphate (Ramirez-Montealegre and Pearce, 2005), was ~40% lower in lysosomes isolated from PS1KO cells relative to WT lysosomes, while ConA treatment of WT cells reduced ATP hydrolysis by ~90%, indicating that, despite the marked loss of V0a1, there is some residual ATPase activity in PS1KO (Figure 4C). Next, we measured the rate of proton translocation into the lysosomal lumen using the quenching of 9-amino-6-chloro-2-methoxyacridine (ACMA), which was ~50% lower in PS1KO lysosomes than in WT lysosomes. As expected, pretreatment of lysosomes with ConA significantly inhibited proton translocation in WT cells, but minimally reduced this rate in PS1KO lysosomes, confirming that loss of PS1 markedly impairs vATPase function (Figure 4D).

### The vATPase V0a1 Subunit Is Essential for Lysosomal Acidification and Autophagic Function

PS1 siRNA treatment of WT cells for 48 hr only partially decreased expression of mature V0a1 and 96 hr of PS1 siRNA was needed to decrease V0a1 levels more than 85% (Figure 5A) and significantly increase LC3-II levels (Figures 5B and 5C),

(E) PS1KO and WT cells transiently transfected for 48 hr with EGFP-mRFP LC3 showed no change in percentages of yellow or red puncta after 0.5 μM Ned-19 for 24 hr.

(F and G) Uptake of lysosome-targeted NP-1 acidic nanoparticles (24 hr, 1 mg/ml) in PS1KO cells restored normal lysosomal pH (F) (n = 6) and lowered ability of ML-SA1 to elevate cytosolic $Ca^{2+}$ (G) (WT, n = 180; PS1KO, n = 186; PS1KO/NP1, n = 237).

(H) NP-1 also elevated lysosomal $Ca^{2+}$ levels (WT, n = 318; PS1KO, n = 305; PS1KO/NP1, n = 313) and lowered cytosolic $Ca^{2+}$ in PS1KO cells (WT, n = 148; PS1KO, n = 150; PS1KO/NP1, n = 150).

(I and J) NP-1 normalized levels of Cat D activity (I), NP-1 reduced yellow puncta (J), and increased red puncta, in PS1KO cells, indicating restored autophagic flux. Scale bars represent 10 μM. *$p < 0.05$, ***/### $p < 0.0001$.

(K) NP-1 increased mature CatD levels and reduced elevated LC3-II/p62 levels in PS1KO cells. Error bars represent ± SEM.

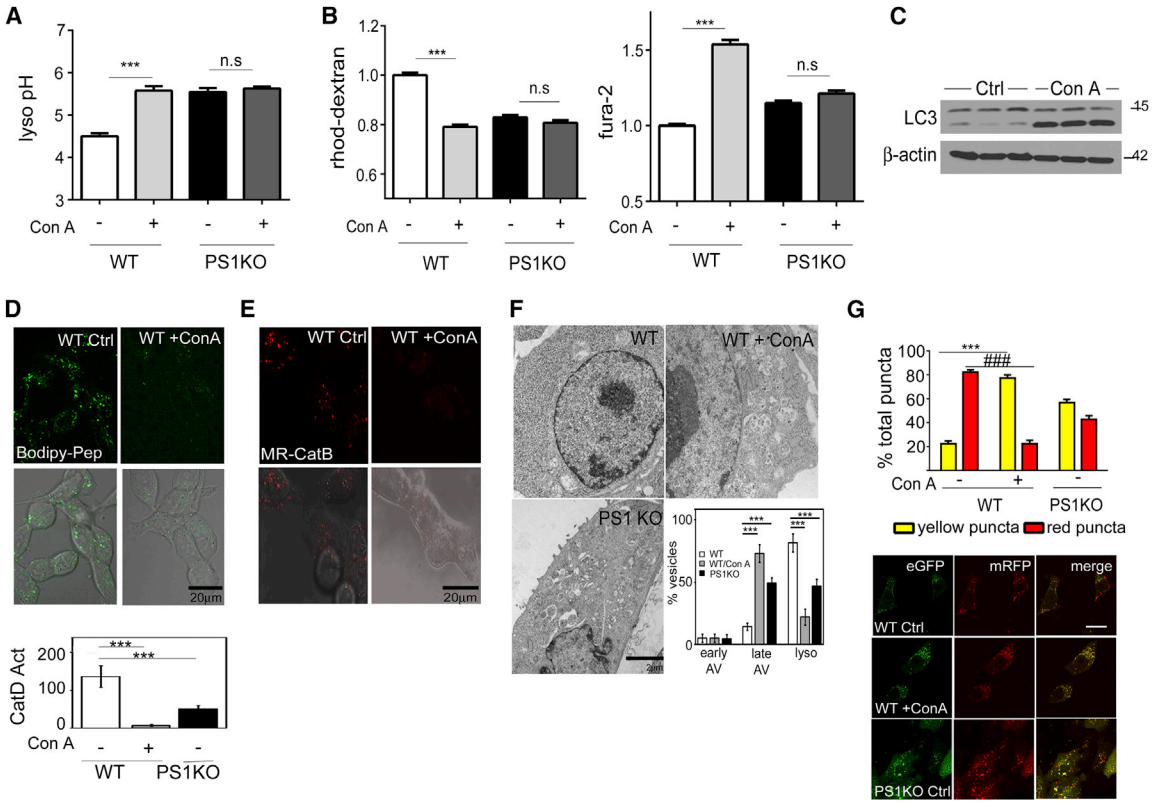


**Figure 3. Inhibition of VATPase Function Induces a PS1KO-like Defective Autophagy Phenotype**

(A) ConA (50 nM, 24 hr) elevated lysosomal pH in WT (n = 6 each), but had no effect on PS1KO cells.

(B) ConA decreased lysosomal $Ca^{2+}$ (WT, n = 155; WT/ConA, n = 153) and elevated cytosolic $Ca^{2+}$ (WT, n = 154; WT/ConA, n = 152) in WT but had no significant effect on $Ca^{2+}$ levels in PS1KO cells (PS1, n = 153 and 164; PS1/ConA, n = 161 and 151, lyso. and cyto.).

(C–F) Con A elevated LC3-II levels (C), decreased in vivo and in vitro CatD enzyme activities and CatB activity (D and E, respectively), and increased late AV accumulation while decreasing lysosome number (F) (n = 25).

(G) ConA (50 nM) elevated yellow puncta and markedly decreased red puncta in EGFP-mRFP-LC3 cells. Scale bars represent 10 μm. *p < 0.05, ***/### p < 0.0001. Error bars represent ± SEM.

indicating diminished lysosomal clearance. LysoTracker signal decreased 50% after 96 hr of V0a1 siRNA (Figure 5D) but only 20% after 48 hr, again underscoring the slow turnover of preexisting V0a1. Similarly, in situ CatB enzyme activity decreased 60% only after 96 hr of V0a1 siRNA exposure (Figure 5E). Thus, even after 4 days of siRNA exposure, residual V0a1 on lysosomes is enough to maintain a minor fraction of normal proton pumping activity. These results support the idea that V0a1 is essential for lysosomal acidification and function and that its turnover is quite long, consistent with previous findings (http://helixweb.nih.gov/ESBL/Database).

## Glycosylation of V0a1 Is Critical for Its Stability and Functions

Glycosylation of the V0a1 subunit has been proposed to influence its stability and function (Gillespie et al., 1991; Lee et al., 2010). It was recently demonstrated that glycosylation of residue R444 in V0a3, an osteoclast-specific V0a isoform, is required for its proper delivery to lysosomes (Bhargava et al., 2012). To investigate the role of glycosylation on the V0a1 subunit, we generated an R447L mutant analogous to the R444L mutation in V0a3, using a C-terminal FLAG-tagged V0a1 (V0a1-FLAG) that enabled the mutant to be differentiated from endogenous V0a1 subunit in murine neuroblastoma (N2a) cells.

To investigate the R447L effects on V0a1 maturation, we treated lysates stably expressing V0a1-FLAG with PNGase F. PNGase converted the mature $V0a1^{WT}$-FLAG to its 100 kDa immature form, whereas there was no discernible shift in the mobility of $V0a1^{R447L}$ after PNGase F treatment. Moreover, levels of $V0a1^{R447L}$ in the stably transfected cells were markedly lower than levels of $V0a1^{WT}$ in the corresponding cells (Figure 6A). To analyze whether this decrease was due to rapid degradation of the unglycosylated protein, cells were treated for 24 hr with the proteasome inhibitor MG-132, and lysates were immunoblotted with anti-FLAG antibody. As predicted, the proteasome inhibitor significantly delayed $V0a1^{R447L}$ degradation (Figure 6B). To document premature turnover of $V0a1^{R447L}$, cells were exposed to cycloheximide for various times. Immunoblot analysis of these lysates confirmed that the glycosylation mutant $V0a1^{R447L}$ is rapidly degraded by the proteasome (Figure 6C). Previous studies demonstrated that immature V0a1 is not correctly delivered to the lysosome but rather retained in the ER (Lee et al.,

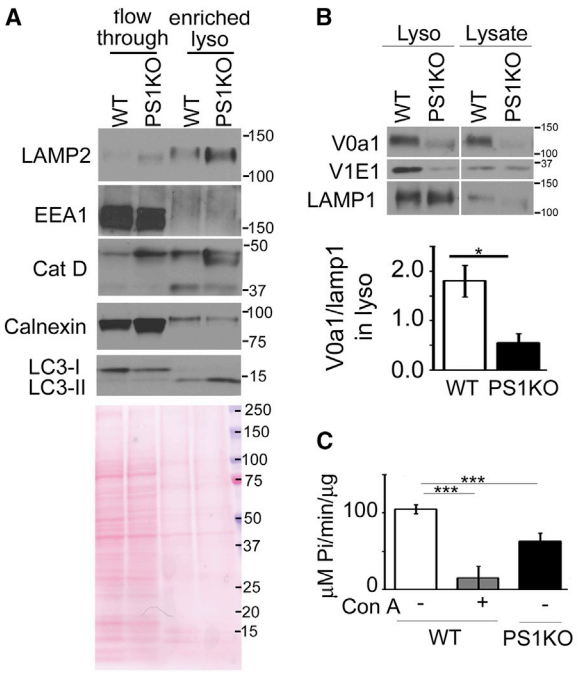


**Figure 4. PS1KO Lysosomes Are Markedly Deficient in vATPase V0a1 Subunit and vATPase Activity**

(A–D) In highly enriched lysosomes from PS1KO cells (A), V0a1 subunit levels were decreased (B) (n = 3), ATP hydrolysis activity was reduced (C), and proton translocation ability of vATPase was decreased (D). ConA treatment of WT cells for 24 hr prior to lysosomal enrichment decreased proton translocation, but had no effect in PS1KO cells. *p < 0.05, ***p < 0.0001. Error bars represent SEM.

2010). To identify the localization of V0a1$^{R447L}$, we fractionated cells on an Opti-prep gradient. Immunoblot analyses of these fractions revealed that V0a1$^{R447L}$ subunit co-sedimented with ER-enriched fractions, whereas V0a1$^{WT}$-FLAG was observed primarily in lysosome-enriched fractions (Figure 6D). Double-immunofluorescence analysis using compartmental markers confirmed the mislocalization of V0a1$^{R447L}$ (Figure 6D).

To further analyze the functional role of V0a1 glycosylation, we incubated V0a1$^{R447L}$ cells with LysoTracker, Bodipy-FL-pepstatin A, and MR-CatB to assay lysosomal acidification and in situ activity of CatD and CatB, respectively. Quantitative analyses demonstrated that both LysoTracker signal and cathepsin activities were significantly decreased in V0a1$^{R447L}$ cells (Figure 6E), commensurate with an observed rise in lysosomal pH and decline in vATPase activity measured directly (Figures 6F and 6G). As expected, levels of autophagy marker protein LC3-II increased (Figure S3A), and clearance of autophagosomes was reduced in V0a1$^{R447L}$ cells (Figure 6H), whereas autophagy induction-related signals (i.e., p-mTOR, p-P70S6K) were not altered (Figure S3B).

These results are in accord with previous findings and establish that V0a1 subunit glycosylation is critical for the stability and lysosomal targeting that enables lysosomal acidification and hydrolytic function.

### PS1 Is an Essential Mediator of Lysosomal Acidification and $Ca^{2+}$ Homeostasis in Neurons

To establish that PS1 loss causes a similar lysosomal phenotype in a neuronal PS1-deficient cell model, we assayed these parameters directly in neurons. Importantly, levels of lysosomal $Ca^{2+}$ were lowered, and cytosolic $Ca^{2+}$ was elevated significantly in PS1KO primary neurons (Figure 7A). Western blot analysis demonstrated that V0a1 maturation is also markedly decreased (Figure 7B). Further indicative of autophagy failure, the numbers of autophagic vacuoles (AVs), consisting of mainly single membrane electron-dense autolysosomes and multilamellar organelles, were significantly increased in neuronal perikarya (Figure 7C). Consistent with abnormally elevated lysosomal pH and disrupted proteolysis, LysoTracker signal and CatB/D activity were significantly decreased in PS1KO neurons compared to WT neurons (Figures 7D–7F), confirming earlier findings in PS1KO cells (Lee et al., 2010). Contrasting with these current findings, Coen et al. (2012) reported no lysosomal acidification deficits in PS1KO neurons. A plausible explanation for their failure to detect differences in neurons lies in the atypical features of the PS1KO neurons they used. In our PS1KO neurons, nicastrin maturation is significantly impaired and APP-CTF levels are increased, as expected from the loss of PS1, and as reported by other groups (Esselens et al., 2004; Wilson et al., 2004), while these signature properties of PS1KO were not present in the neurons used by Coen et al. (2012).

## DISCUSSION

Presenilin 1 plays an important role in $Ca^{2+}$ homeostasis and autophagy/lysosomal protein degradation, beyond its well-studied catalytic role as part of γ-secretase (Lee et al., 2010; Tu et al., 2006). However, the relationship between two major γ-secretase independent functions of PS1, namely maintenance of $Ca^{2+}$ homeostasis and lysosomal proteolysis, is poorly understood. Based on an earlier observation that lysosomal alkalinization increased lysosomal $Ca^{2+}$ efflux (Christensen et al., 2002), it was reasonable to suspect that lysosomal acidification failure resulting from loss of PS1 may also disrupt lysosomal $Ca^{2+}$ homeostasis. In this study, we show that acidic lysosomal pH is indeed essential for maintaining normal lysosomal $Ca^{2+}$ levels, whereas restoration of lysosomal $Ca^{2+}$ levels by itself does not significantly affect lysosomal acidification under these conditions. Our direct measurements reveal significantly decreased lysosomal $Ca^{2+}$ in PS1 ablated cells and neurons. Additional measurements of lysosomal $Ca^{2+}$ levels after GPN-mediated lysosome rupture and $Ca^{2+}$ release confirm the lysosomal $Ca^{2+}$ deficit. Notably, we also demonstrate that TRPML1-mediated release of lysosomal $Ca^{2+}$ in PS1KO cells

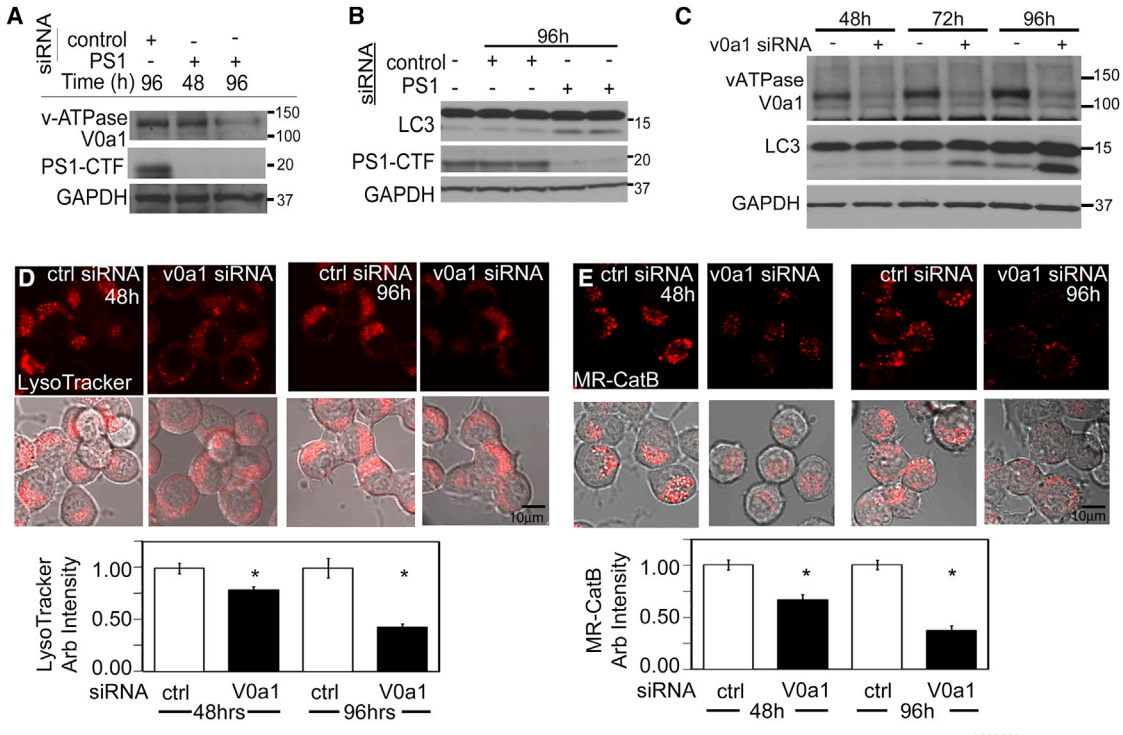


**Figure 5. vATPase V0a1 Knockdown Inhibits Lysosomal Acidification**

(A and B) PS1 siRNA in WT cells decreased V0a1 levels (A) and increased LC3-II (B).

(C–E) Levels of LC3-II were increased after V0a1 subunit siRNA treatment (C). LysoTracker intensity (n = 55) (D) and CatB activity (n = 30) (E) decreased after V0a1 siRNA. Scale bars represents 10 μm. *p < 0.05. Error bars represent SEM.

substantially increases cytosolic $Ca^{2+}$ levels and is a major contributor to the PS1-related $Ca^{2+}$ defect previously attributed only to disruption of ER $Ca^{2+}$ homeostasis (Chan et al., 2000; Cheung et al., 2010).

Increasing evidence suggests that the primary $Ca^{2+}$ stores targeted by NAADP are present in acidic organelles such as the lysosome and are distinct from pools in the ER (Calcraft et al., 2009). TPC2 is the primary NAADP-dependent $Ca^{2+}$ efflux channel in the lysosome, and its activation via NAADP has previously been shown to be sensitive to lysosomal pH. In fully acidified lysosomes, $Ca^{2+}$ stores that are lowered by elevated NAADP levels become replenished when the dissociation rate between NAADP and TPC2 increases (Pitt et al., 2010). When lysosomal pH is normal, elevated cytosolic NAADP levels induce lysosomal $Ca^{2+}$ release from lysosomal stores (Churchill et al., 2002; Lloyd-Evans et al., 2008). However, increasing lysosomal pH leads to a failure of the purified TPC2 to dissociate from NAADP, rendering the channel inactive (Pitt et al., 2010).

PS1KO cells, which have elevated lysosomal pH, treated with NAADP-AM did not release lysosomal $Ca^{2+}$, whereas U1866a-treated WT cells, possessing a normal lysosomal pH, released lysosomal $Ca^{2+}$ in response to NAADP-AM treatment (Lloyd-Evans et al., 2008). These data are consistent with the TPC2 channel being inactive in PS1KO cells. Conversely, ML-SA1, an agonist for the lysosomal TRPML1 channel, evoked a stronger release of $Ca^{2+}$ in PS1KO cells than in WT cells, despite the lower lysosomal $Ca^{2+}$ content in PS1KO cells.

Our data indicate that TRPML1 in PS1KO cells is more responsive to low concentrations of the agonist, ML-SA1, and likely exists in a hyperactive state. In addition, there have been reports that endogenous TRPML1, as opposed to a constitutively active mutant form of TRPML1 overexpressed in cells (Dong et al., 2009), is less active at a lower pH range and becomes more active as pH increases (Raychowdhury et al., 2004). This property of the channel appears to contribute to its hyperactivity at elevated lysosomal pH in PS1KO cells. To establish that TRPML1, the lysosomally localized member of the TRPML family, is the primary $Ca^{2+}$ efflux channel and is specifically activated by elevated lysosomal pH, we showed that TRPML1 knockdown in PS1KO cells elevates lysosomal $Ca^{2+}$ and decreases cytosolic $Ca^{2+}$ and that an inhibitory antibody against TRPML1 abolishes ML-SA1-mediated lysosomal $Ca^{2+}$ release. In addition, cytosolic $Ca^{2+}$ did not rise when ML-SA1-treated control and MLIV fibroblasts were pretreated with GPN to abolish any $Ca^{2+}$ signal from lysosomal stores, implying a principal lysosomal source for this cytosolic $Ca^{2+}$ rise. Moreover, we observed a large increase in cytosolic $Ca^{2+}$ in ConA-treated control fibroblasts, indicating that inhibition of vATPase and thus an elevation of lysosomal pH can induce TRPML1 sensitivity to ML-SA1. Additionally, pretreatment of PS1KO cells with NP-1 to lower lysosomal pH normalized the rise in cytosolic $Ca^{2+}$ mediated by ML-SA1 as observed in untreated cells.

Ned-19 normalized the abnormal ML-SA1-induced $Ca^{2+}$ release in the PS1KO cells, providing additional evidence that

the increased $Ca^{2+}$ efflux is due to hyperactive TRPML1. By blocking lysosomal $Ca^{2+}$ leak, Ned-19 restored $Ca^{2+}$ homeostasis in PS1KO cells, but had no detectable effect on lysosomal pH or any aspect of the abnormal lysosomal/autophagy phenotype in PS1KO cells. If lysosomal $Ca^{2+}$ fluxes were a significant influence on lysosomal acidification, we would have expected Ned-19 treatment to alter the elevated lysosomal pH in PS1KO cells. In addition, ConA recapitulated PS1KO phenotypes in WT cells but, as expected, did not worsen the $Ca^{2+}$ defect in PS1KO cells. Thus, our data provide strong evidence that elevated lysosomal pH is the basis for both reduced lysosomal $Ca^{2+}$ and lysosomal/autophagy defects in PS1KO cells.

In AD, ER $Ca^{2+}$ homeostasis is dysregulated and multiple $Ca^{2+}$ regulatory mechanisms, including inositol 1,4,5-triphosphate and ryanodine receptors, are known to be disrupted by PS1 loss of function in early onset AD (Chan et al., 2000; Cheung et al., 2010), leading to an increase in cytosolic $Ca^{2+}$. Interestingly, lysosomal $Ca^{2+}$ release can trigger secondary ER $Ca^{2+}$ release via nanojunctions (Fameli et al., 2014; Kilpatrick et al., 2013). Possible crosstalk between ER and lysosomal $Ca^{2+}$ fluxes, however, has not been fully considered in AD pathogenesis. Our current data raise the possibility that lysosomal $Ca^{2+}$ release or leak driven by lysosomal acidification deficits could promote ER $Ca^{2+}$ dysregulation, in addition to directly elevating cytosolic $Ca^{2+}$ levels. The findings show a role of both pH and lysosomal $Ca^{2+}$ leak in maintaining normal lysosomal $Ca^{2+}$ levels and a capability of lysosomal $Ca^{2+}$ leak to alter cytosolic $Ca^{2+}$ levels substantially.

Lysosomal acidification is maintained primarily by the vATPase, a protein complex composed of a membrane-bound V0 domain and a peripherally associated V1 domain. The largest subunit of the V0 sub-complex, V0a, is an integral membrane protein with four known isoforms (a1–a4), a1 being the major one in brain (Nishi and Forgac, 2000). We demonstrated previously that PS1 deletion, PS1/2 deletion, or FAD-related mutation of PS1 reduces vATPase immunoreactivity on lysosomes, elevates lysosomal pH, depresses lysosomal protease activation, and significantly delays autophagic protein turnover. Moreover, stable transfection of PS1 into PS1/2 DKO cells reverses these features and restores V0a1 subunit glycosylation, lysosomal acidification, and autophagic clearance (Lee et al., 2010). Importantly, additional studies have also demonstrated impaired vATPase V0a1 subunit maturation and endolysosomal acidification in multiple models, including PS1 ablated cells or mutant PS1 models (Avrahami et al., 2013; Coffey et al., 2014; Dobrowolski et al., 2012; Torres et al., 2012; Wolfe et al., 2013), underscoring that the acidification defect induced by PS1 loss of function is generalizable across various cell types. In one study, PS1 and vATPase V0a1 subunit were reported to have no role in lysosomal pH regulation (Coen et al., 2012), and differences between methods and cell culture conditions might explain some discrepancies between this study and studies by us and others. In our current study, we show that lysosomes purified from PS1KO cells contained markedly lowered levels of V0a1 subunit, which was associated with impaired vATPase assembly on lysosomes and commensurate reductions of lysosomal proton pumping activity. Using siRNA gene knockdown, we further demonstrated that lysosomal acidification and lysosomal enzyme activation require the vATPase V0a1 subunit, in agreement with other findings that V0a1 subunit is critical for vesicular acidification (Raines et al., 2013; Saw et al., 2011). Notably, V0a1 has a long half-life on lysosomes, requiring substantial duration of siRNA exposure (96 hr) to lower lysosomal levels of the subunit sufficiently to alter acidification, which is 48 hr longer than the interval used in the Coen et al. (2012) study where a pH change could not be detected upon siRNA treatment. We observed that the glycosylation mutant $V0a1^{R447L}$ stably expressed in cells exhibited increased ER retention, decreased stability promoting loss via ERAD, and deficient lysosomal targeting and assembly. Without proper maturation of the V0a1 glycosylation mutant, lysosomal acidification and functions, including lysosomal enzyme activation and autophagic cargo degradation, were impaired. These findings strongly support the conclusion that both the expression and proper glycosylation of V0a1 are critical for its lysosomal function.

Our data also establish that defective lysosomal acidification is the essential factor accounting for the abnormal autophagy/lysosomal degradation and lysosomal $Ca^{2+}$ phenotypes in PS1 deficient neurons and non-neural cells. ConA inhibition of the vATPase in WT cells reproduced all of the features of the PS1KO phenotype, whereas Ned-19 corrected lysosomal $Ca^{2+}$ levels without influencing lysosomal pH deficits or other aspects of autophagy dysfunction. Most importantly, we were able to reverse both autophagy and lysosomal $Ca^{2+}$ deficits specifically by re-acidifying lysosomes using a form of lysosome-targeted acidic nanoparticles previously shown to restore lysosomal pH in ARPE 19 cells, a model of macular degeneration (Baltazar et al., 2012).

In conclusion, we have shown that the vATPase V0a1 subunit is essential for lysosomal acidification and that its maturation and proper functional assembly on lysosomes require PS1. Moreover, we have established that lysosomal $Ca^{2+}$ homeostasis is modulated by lysosomal pH and that the abnormal TRPML1 mediated efflux of $Ca^{2+}$ from lysosomes induced by PS1 deletion is a secondary consequence of impaired lysosomal acidification caused by inadequate levels of vATPase activity. Substantial evidence suggests that both the lysosomal/autophagic and calcium homeostasis abnormalities induced by PS1 loss of function are likely to contribute significantly to disease pathogenesis in this familial form of AD, as well as in late-onset AD where similar pathobiology develops possibly via different initiating factors (Nixon and Yang, 2011). Restoration of autophagy/lysosomal function in PS1-deficient cells by reacidifying lysosomes suggests innovative approaches to therapy for AD and other neuropathological conditions associated with lysosomal pH elevation.

## EXPERIMENTAL PROCEDURES

Methods are described in detail in the Supplemental Experimental Procedures.

### Cell Lines and Reagents

Murine blastocysts with different PS1 genotypes (WT, BD6; PS1KO, BD15) were previously characterized (Lee et al., 2010). Control and MLIV human fibroblasts were purchased from Coriell Cell Repository and have numbers GM005399 and GM002527, respectively, and were maintained in 10% fetal

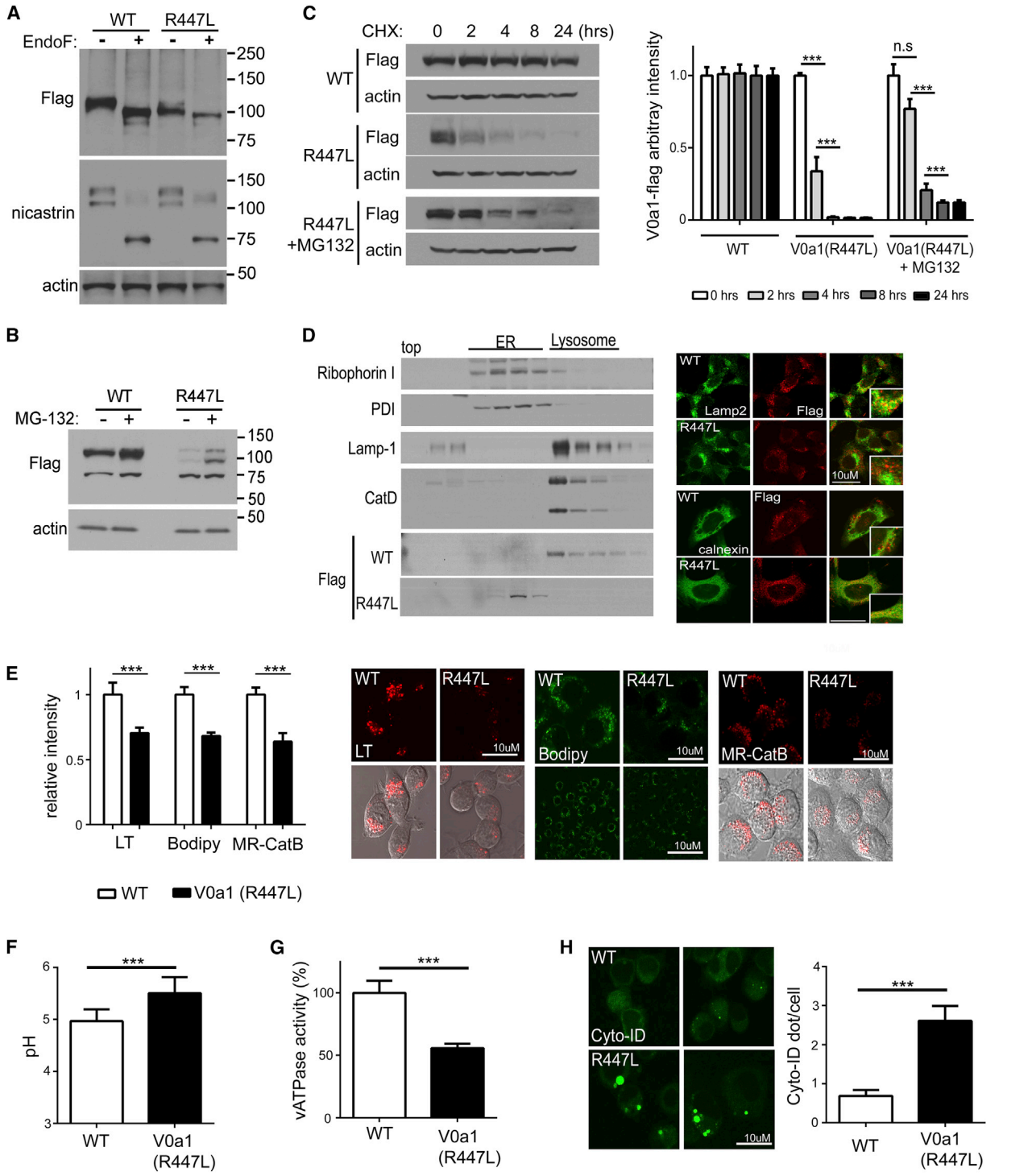


**Figure 6. The Mutant Protein Construct V0a1$^{R447L}$-FLAG Is Not Glycosylated and Is Degraded in N2a Cells**

(A) Cell lysates were immunoblotted with anti-FLAG antibody followed by PNGase F treatment. Nicastrin blots provided as a positive control for PNGase treatments.

(B and C) Cell lysates were immunoblotted with anti-FLAG antibody followed by proteasome inhibitor (B) (MG-132) treatment for 24 hr (C). Cell lysates were immunoblotted with anti-FLAG antibody followed by CHX treatment for the indicated time. Cell lysates form V0a1$^{R447L}$-FLAG were preincubated with MG-132 for 24 hr then treated with CHX for the indicated time. Levels of V0a1-FLAG were quantified. Results were plotted as ratios normalized to the non-treated sample for each cell line.

*(legend continued on next page)*

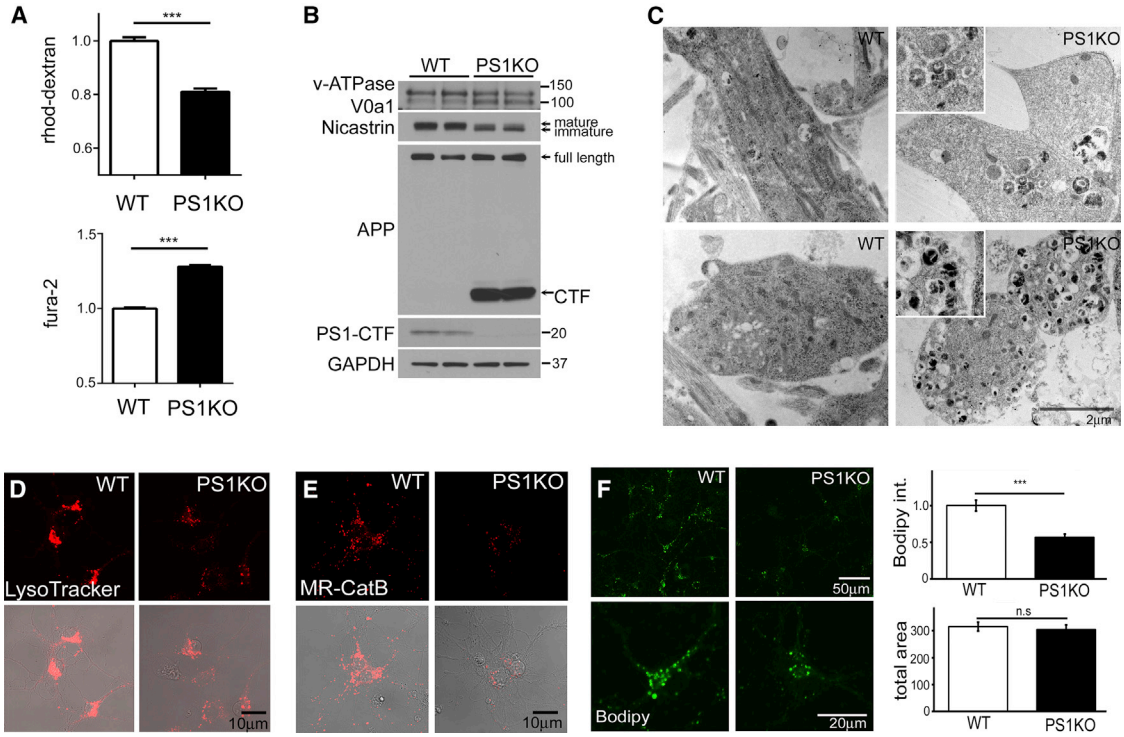


**Figure 7. Lysosomal $Ca^{2+}$, Acidification, and Enzyme Activities Are Reduced in PS1KO Neurons**

(A) Lysosomal $Ca^{2+}$ (WT, n = 180; PS1KO, n = 181) was reduced, and cytosolic $Ca^{2+}$ (n = 20) was elevated in PS1KO neurons.

(B–F) In PS1KO neurons, maturation of V0a1 and nicastrin was decreased, and APP-CTF levels were increased (B). AVs accumulate in both cell bodies and axons (C). LysoTracker signal (D) and in vivo CatB (E) and CatD (n = 28) (F) activities were decreased. Scale bars represents 10 μm. ***$p < 0.0001$. Error bars represents SEM.

bovine serum (FBS) in DMEM with 5% $CO_2$. Murine neuroblastoma (N2A) cells were maintained in DMEM with penicillin/streptomycin and 10% FBS at 37°C and 5% $CO_2$. Mouse PS1 (MSS208049) and scramble (12935-200) siRNA were purchased from Invitrogen and mouse vATPase V0a1 siRNA (11975) from Thermo Scientific. Cells were transfected using Lipofectamine RNAiMAX (Invitrogen). Primary cortical neuronal culture were derived from E15 stage pups from PS1 (+/−) crosses and cultured with Neurobasal medium. These experiments were performed according to "Principles of Animal Care" (NIH, 1985) and approved by the Institutional Animal Care and Use Committee at the Nathan Kline Institute.

A musculus v-ATPase $V0a1^{WT}$-FLAG construct (EX-Mn20338-M13) was purchased from GeneCopoeia. A $V0a1^{R447L}$-FLAG mutant DNA construct was generated using a QuikChange II XL site-directed mutagenesis kit (Agilent technologies, #200521) according to manufacturer's instructions with 5′-GCATGGTGTTCAGCGGCCTATACATTATTCTTCTGATG-3′ and 5′-CATCAG AAGAATAATGTATAGGCCGCTGAACACCATGC-3′ primer set. After establishing the stable cell line, cells were maintained with G418 (300 μg/ml)-containing medium.

Either GFP-shTPCN2 or GFP-shTRPML1 (QIAGEN) were transfected with Lipofectamine 2000 (Invitrogen) for 72 hr, and calcium measurements for cells containing the GFP signal were calculated for either cytosolic or lysosomal $Ca^{2+}$.

### Gel Electrophoresis, Immunoblotting, and Confocal Laser Scanning Microscopy

Experiments were performed as previously described (Lee et al., 2010).

### Deglycosylation and Cycloheximide Treatment

To assess FLAG-tagged V0a1 mutant glycosylation, samples were treated for 24 hr at 37°C with PNGase F using an enzymatic deglycosylation kit according to the manufacturer's instruction (PROzyme). To assess the stability of the V0a1 mutant, samples were treated with CHX (100 μg/ml) for 0, 2, 4, 8, and 24 hr with or without pretreatment with MG-132 (1 μM/ml, 24 hr) and then analyzed by SDS-PAGE.

### Subcellular Fractionation and Enzyme Activity for Cathepsins

Procedures were performed as previously described (Lee et al., 2010).

(D) Immunoblot of V0a1-FLAG distribution in subcellular fractions of $V0a1^{WT}$-FLAG and $V0a1^{R447L}$-FLAG. ER marker proteins (Ribophorin-I and PDI) primary localized in fractions 5–11 and lysosomal marker proteins (LAMP-1 and mature CatD) mainly in fractions 13–17. Double immunostaining showed strong colocalization of V0a1-FLAG and LAMP-2 in $V0a1^{WT}$ -FLAG cells, whereas $V0a1^{R447L}$-FLAG strongly colocalized with ER marker calnexin. Scale bar represents 10 μm.

(E) Cells were incubated with LysoTracker for lysosomal acidification assay. To access the in vivo lysosomal enzyme activity, cells were incubated with Bodipy-FL-pepstatin A and MR-CatB for CatD and CatB activity, respectively. Scale bar represents 10 μm. Intensity of signal was quantified (LT, n = 60; Bodipy, n = 50; MR-CatB, n = 55). Results were plotted as ratios normalized to $V0a1^{WT}$-FLAG.

(F) Lysosomal pH values were measured ratiometrically using LysoSensor Yellow/Blue-dextran (n = 10, at least $6 \times 10^3$ cells/n).

(G) v-ATPase activity was reduced in $V0a1^{R447L}$cells.

(H) Autophagosomes were immunolabeled with Cyto-ID autophagy detection kit. Results were plotted as mean of AV (Cyto-ID) puncta number per cells (n = 80). Scale bar represents 10 μm. *$p < 0.05$, **$p < 0.001$, ***$p < 0.0001$. Error bars represent ± SEM.

### Lysosomal pH Measurement and Ultrastructural Analyses

Procedures were performed as previously described (Wolfe et al., 2013).

### Lysosomal Isolation

Cells were incubated in growth medium containing 1 mM HEPES (pH 7.2) and 10% Dextran-conjugated magnetite (Liquid Research LLC) for 24 hr and then chased in normal growth media for 24 hr. Cells were washed in PBS then harvested in 4 ml of ice-cold Buffer A. Cells were then homogenized with 40 strokes of a tight-fitting pestle in a Dounce homogenizer then passed through a 22G needle five times. After homogenization, 500 μl of ice-cold Buffer B (220 mM HEPES, 375 mM KCL, 22.5 mM MgAc, 1 mM DTT, DNase I) was added and samples were then centrifuged at 750 × *g* for 10 min. The supernatant was then decanted over a QuadroMAC LS column that had previously been equilibrated with 0.5% BSA in PBS. The pellet was subjected to re-addition of 4 ml cold Buffer A and 500 μl cold Buffer B and then resuspended and recentrifuged. DNase I (10 μl/ml in PBS) was added, and the column was then incubated for 10 min and then washed with 1 ml cold PBS. Lysosomes were eluted by removing the column from the magnetic assembly, adding 500 μl of PBS and forced through the column using a plunger.

### vATPase Activity Assay

Lysosome-enriched fractions were mixed with 3 vol of Buffer and incubated at 37°C for 5 min. After incubation, the reaction was started by addition of 2 mM ATP and incubated 20 min at 37°C. The ATPase reaction was stopped after 25 min by the addition of 2 ml of molybdate solution and 0.2 ml of ascorbic acid and then developed for 5 min at room temperature. Control samples were measured in the presence of the vATPase inhibitor ConA (1 μM), and the experimental values were subtracted accordingly. Absorbance was measured at 750 nm, and solutions of $KH_2PO_4$ were used to generate a standard curve.

### Proton Translocation Assay

Proton transport activity into the lumen of isolated lysosomes was measured by fluorescence quenching of ACMA in the presence or absence of 1 μM concanamycin A. Lysosomes were added to a cuvette containing 2 ml of reaction buffer. The reaction was started by the addition of 1 mM ATP in BTP (pH 7.5), a measurement (ex412/em480) taken every 5 s for 600 s on a SpectraMax M5 multimode reader (Molecular Devices).

### Lysosomal $Ca^{2+}$ Measurements

Cells were plated on glass bottom dishes the night before treatment. For baseline calcium measurements, cells were incubated with 25 mg/ml rhod-dextran for 12 hr before imaging. For all cytosolic measurements, cells were incubated with either 5 μM Oregon-Green 488 Bapta-1 AM (Life Technologies) or 2 μM Fura-2 AM (Life Technologies) for 1 hr and then chased with complete medium for 30 min. Cells were washed with HBSS (Invitrogen) and imaged and analyzed using ImageJ (NIH).

Release of lysosomal $Ca^{2+}$ was measured using methods adapted from those previously described (Lloyd-Evans et al., 2008). Cells were plated on μ-Slide eight-well imaging dishes (ibidi), left to adhere overnight and then treated with 2 μg/ml U18666a for 24 hr as appropriate. Postincubation, cells were loaded with either 5 μM Fluo3-AM or 5 μM Fura 2-AM (StratechScientific LTD) in DMEM with 1% BSA and 0.0025% Pluronic acid F127 for 1 hr at 37°C and then washed, left for 10 min to allow deesterification of the calcium dye, and imaged in 1× HBSS with 1 mM HEPES, 1 mM $MgCl_2$, and 1 mM $CaCl_2$. $Ca^{2+}$-free HBSS was used for all human fibroblast experiments. Intracellular $Ca^{2+}$ responses were recorded using a Zeiss Colibri LED microscope system with an AxiocamMrm CCD camera and Zeiss Axiovision software version 4.7 with the additional physiology module for live cell $Ca^{2+}$ imaging.

### Acidic Nanoparticle Treatment

PLGA ResomerH RG 502 H was purchased from Boerhinger Ingelheim and prepared as previously described (Baltazar et al., 2012).

### Analytical Procedures

Quantitative colocalization analysis was performed using ImageJ software (NIH Image), and all experiments were performed in triplicate unless otherwise indicated. Error bars represent ± SEM.

## SUPPLEMENTAL INFORMATION

Supplemental Information includes Supplemental Experimental Procedures and three figures and can be found with this article online at http://dx.doi.org/10.1016/j.celrep.2015.07.050.

## AUTHOR CONTRIBUTIONS

J.-H.L. performed experiments in Figures 5, 6, and 7. M.K.M. performed experiments in Figures 1, 2, 3, and 7. D.M.W. performed experiments in Figures 2, 3, and 4. L.J.H. and E.L.-E. performed experiments in Figure 1. A.K. performed EM analysis. Y.S. and P.P.Y.L. established primary neuron cultures. P.M. performed in vitro CatD activity assays. U.K. and C.H.M. contributed acid nanoparticles and guidance on their use. E.E.C. assisted in nanoparticle experiments. J.-H.L., M.K.M., D.M.W., L.J.H., E.L.-E., and R.A.N. designed experiments, analyzed data, and wrote the paper.

## ACKNOWLEDGMENTS

We are very grateful to Dr. Alan Bernstein (Global HIV Vaccine Enterprise) for PS BD cells. The authors also thank Nicole Gogel for assisting in manuscript preparation and Cori Peterhoff for assisting in formatting figures. This work was supported by NIH P01AG017617, Takeda Pharmaceutical Company, New York Community Trust, and Litwin Foundation, Inc., to R.A.N. The work was also supported by a RCUK Fellowship and Royal Society grant to E.L.E. and BBRSC PhD and MRC in vivo skills award funding support to L.-J.H. U.K. is a co-founder and shareholder of Ocugen, Inc., and EyeTrans Technologies, Inc.

Received: September 10, 2014
Revised: April 22, 2015
Accepted: July 24, 2015
Published: August 20, 2015

## REFERENCES

Avrahami, L., Farfara, D., Shaham-Kol, M., Vassar, R., Frenkel, D., and Eldar-Finkelman, H. (2013). Inhibition of glycogen synthase kinase-3 ameliorates β-amyloid pathology and restores lysosomal acidification and mammalian target of rapamycin activity in the Alzheimer disease mouse model: in vivo and in vitro studies. J. Biol. Chem. *288*, 1295–1306.

Baltazar, G.C., Guha, S., Lu, W., Lim, J., Boesze-Battaglia, K., Laties, A.M., Tyagi, P., Kompella, U.B., and Mitchell, C.H. (2012). Acidic nanoparticles are trafficked to lysosomes and restore an acidic lysosomal pH and degradative function to compromised ARPE-19 cells. PLoS ONE *7*, e49635.

Bhargava, A., Voronov, I., Wang, Y., Glogauer, M., Kartner, N., and Manolson, M.F. (2012). Osteopetrosis mutation R444L causes endoplasmic reticulum retention and misprocessing of vacuolar H+-ATPase a3 subunit. J. Biol. Chem. *287*, 26829–26839.

Butler, D., Hwang, J., Estick, C., Nishiyama, A., Kumar, S.S., Baveghems, C., Young-Oxendine, H.B., Wisniewski, M.L., Charalambides, A., and Bahr, B.A. (2011). Protective effects of positive lysosomal modulation in Alzheimer's disease transgenic mouse models. PLoS ONE *6*, e20501.

Calcraft, P.J., Ruas, M., Pan, Z., Cheng, X., Arredouani, A., Hao, X., Tang, J., Rietdorf, K., Teboul, L., Chuang, K.T., et al. (2009). NAADP mobilizes calcium from acidic organelles through two-pore channels. Nature *459*, 596–600.

Česen, M.H., Pegan, K., Spes, A., and Turk, B. (2012). Lysosomal pathways to cell death and their therapeutic applications. Exp. Cell Res. *318*, 1245–1251.

Chan, S.L., Mayne, M., Holden, C.P., Geiger, J.D., and Mattson, M.P. (2000). Presenilin-1 mutations increase levels of ryanodine receptors and calcium release in PC12 cells and cortical neurons. J. Biol. Chem. *275*, 18195–18200.

Chávez-Gutiérrez, L., Bammens, L., Benilova, I., Vandersteen, A., Benurwar, M., Borgers, M., Lismont, S., Zhou, L., Van Cleynenbreugel, S., Esselmann, H., et al. (2012). The mechanism of γ-Secretase dysfunction in familial Alzheimer disease. EMBO J. *31*, 2261–2274.

Cheung, K.H., Mei, L., Mak, D.O., Hayashi, I., Iwatsubo, T., Kang, D.E., and Foskett, J.K. (2010). Gain-of-function enhancement of IP3 receptor modal gating by familial Alzheimer's disease-linked presenilin mutants in human cells and mouse neurons. Sci. Signal. *3*, ra22.

Christensen, K.A., Myers, J.T., and Swanson, J.A. (2002). pH-dependent regulation of lysosomal calcium in macrophages. J. Cell Sci. *115*, 599–607.

Churchill, G.C., Okada, Y., Thomas, J.M., Genazzani, A.A., Patel, S., and Galione, A. (2002). NAADP mobilizes Ca(2+) from reserve granules, lysosome-related organelles, in sea urchin eggs. Cell *111*, 703–708.

Coen, K., Flannagan, R.S., Baron, S., Carraro-Lacroix, L.R., Wang, D., Vermeire, W., Michiels, C., Munck, S., Baert, V., Sugita, S., et al. (2012). Lysosomal calcium homeostasis defects, not proton pump defects, cause endo-lysosomal dysfunction in PSEN-deficient cells. J. Cell Biol. *198*, 23–35.

Coffey, E.E., Beckel, J.M., Laties, A.M., and Mitchell, C.H. (2014). Lysosomal alkalization and dysfunction in human fibroblasts with the Alzheimer's disease-linked presenilin 1 A246E mutation can be reversed with cAMP. Neuroscience *263*, 111–124.

De Strooper, B., and Annaert, W. (2010). Novel research horizons for presenilins and γ-secretases in cell biology and disease. Annu. Rev. Cell Dev. Biol. *26*, 235–260.

Dobrowolski, R., Vick, P., Ploper, D., Gumper, I., Snitkin, H., Sabatini, D.D., and De Robertis, E.M. (2012). Presenilin deficiency or lysosomal inhibition enhances Wnt signaling through relocalization of GSK3 to the late-endosomal compartment. Cell Rep. *2*, 1316–1328.

Dong, X.P., Wang, X., Shen, D., Chen, S., Liu, M., Wang, Y., Mills, E., Cheng, X., Delling, M., and Xu, H. (2009). Activating mutations of the TRPML1 channel revealed by proline-scanning mutagenesis. J. Biol. Chem. *284*, 32040–32052.

Dong, X.P., Shen, D., Wang, X., Dawson, T., Li, X., Zhang, Q., Cheng, X., Zhang, Y., Weisman, L.S., Delling, M., and Xu, H. (2010). PI(3,5)P(2) controls membrane trafficking by direct activation of mucolipin Ca(2+) release channels in the endolysosome. Nat. Commun. *1*, 38.

Esselens, C., Oorschot, V., Baert, V., Raemaekers, T., Spittaels, K., Serneels, L., Zheng, H., Saftig, P., De Strooper, B., Klumperman, J., and Annaert, W. (2004). Presenilin 1 mediates the turnover of telencephalin in hippocampal neurons via an autophagic degradative pathway. J. Cell Biol. *166*, 1041–1054.

Fameli, N., Ogunbayo, O.A., van Breemen, C., and Evans, A.M. (2014). Cytoplasmic nanojunctions between lysosomes and sarcoplasmic reticulum are required for specific calcium signaling. F1000Res. *3*, 93.

Frakes, A.E., Ferraiuolo, L., Haidet-Phillips, A.M., Schmelzer, L., Braun, L., Miranda, C.J., Ladner, K.J., Bevan, A.K., Foust, K.D., Godbout, J.P., et al. (2014). Microglia induce motor neuron death via the classical NF-κB pathway in amyotrophic lateral sclerosis. Neuron *81*, 1009–1023.

Ghavami, S., Shojaei, S., Yeganeh, B., Ande, S.R., Jangamreddy, J.R., Mehrpour, M., Christoffersson, J., Chaabane, W., Moghadam, A.R., Kashani, H.H., et al. (2014). Autophagy and apoptosis dysfunction in neurodegenerative disorders. Prog. Neurobiol. *112*, 24–49.

Gillespie, J., Ozanne, S., Tugal, B., Percy, J., Warren, M., Haywood, J., and Apps, D. (1991). The vacuolar H(+)-translocating ATPase of renal tubules contains a 115-kDa glycosylated subunit. FEBS Lett. *282*, 69–72.

Grimm, C., Jörs, S., Saldanha, S.A., Obukhov, A.G., Pan, B., Oshima, K., Cuajungco, M.P., Chase, P., Hodder, P., and Heller, S. (2010). Small molecule activators of TRPML3. Chem. Biol. *17*, 135–148.

Jha, A., Ahuja, M., Patel, S., Brailoiu, E., and Muallem, S. (2014). Convergent regulation of the lysosomal two-pore channel-2 by $Mg^{2+}$, NAADP, $PI(3,5)P_2$ and multiple protein kinases. EMBO J. *33*, 501–511.

Kang, D.E., Soriano, S., Frosch, M.P., Collins, T., Naruse, S., Sisodia, S.S., Leibowitz, G., Levine, F., and Koo, E.H. (1999). Presenilin 1 facilitates the constitutive turnover of beta-catenin: differential activity of Alzheimer's disease-linked PS1 mutants in the beta-catenin-signaling pathway. J. Neurosci. *19*, 4229–4237.

Kilpatrick, B.S., Eden, E.R., Schapira, A.H., Futter, C.E., and Patel, S. (2013). Direct mobilisation of lysosomal Ca2+ triggers complex Ca2+ signals. J. Cell Sci. *126*, 60–66.

Lee, J.H., Yu, W.H., Kumar, A., Lee, S., Mohan, P.S., Peterhoff, C.M., Wolfe, D.M., Martinez-Vicente, M., Massey, A.C., Sovak, G., et al. (2010). Lysosomal proteolysis and autophagy require presenilin 1 and are disrupted by Alzheimer-related PS1 mutations. Cell *141*, 1146–1158.

Lloyd-Evans, E., Morgan, A.J., He, X., Smith, D.A., Elliot-Smith, E., Sillence, D.J., Churchill, G.C., Schuchman, E.H., Galione, A., and Platt, F.M. (2008). Niemann-Pick disease type C1 is a sphingosine storage disease that causes deregulation of lysosomal calcium. Nat. Med. *14*, 1247–1255.

Menzies, F.M., Fleming, A., and Rubinsztein, D.C. (2015). Compromised autophagy and neurodegenerative diseases. Nat. Rev. Neurosci. *16*, 345–357.

Mindell, J.A. (2012). Lysosomal acidification mechanisms. Annu. Rev. Physiol. *74*, 69–86.

National Institutes of Health (1985). Health Research Extension Act of 1985, Public Law 99-158, November 20, 1985, Animals in Research. http://grants.nih.gov/grants/olaw/references/phspol.htm.

Naylor, E., Arredouani, A., Vasudevan, S.R., Lewis, A.M., Parkesh, R., Mizote, A., Rosen, D., Thomas, J.M., Izumi, M., Ganesan, A., et al. (2009). Identification of a chemical probe for NAADP by virtual screening. Nat. Chem. Biol. *5*, 220–226.

Nishi, T., and Forgac, M. (2000). Molecular cloning and expression of three isoforms of the 100-kDa a subunit of the mouse vacuolar proton-translocating ATPase. J. Biol. Chem. *275*, 6824–6830.

Nixon, R.A. (2007). Autophagy, amyloidogenesis and Alzheimer disease. J. Cell Sci. *120*, 4081–4091.

Nixon, R.A. (2013). The role of autophagy in neurodegenerative disease. Nat. Med. *19*, 983–997.

Nixon, R.A., and Yang, D.S. (2011). Autophagy failure in Alzheimer's disease–locating the primary defect. Neurobiol. Dis. *43*, 38–45.

Nixon, R.A., and Yang, D.S. (2012). Autophagy and neuronal cell death in neurological disorders. Cold Spring Harb. Perspect. Biol. *4*, a008839.

Penny, C.J., Kilpatrick, B.S., Han, J.M., Sneyd, J., and Patel, S. (2014). A computational model of lysosome-ER Ca2+ microdomains. J. Cell Sci. *127*, 2934–2943.

Pitt, S.J., Funnell, T.M., Sitsapesan, M., Venturi, E., Rietdorf, K., Ruas, M., Ganesan, A., Gosain, R., Churchill, G.C., Zhu, M.X., et al. (2010). TPC2 is a novel NAADP-sensitive Ca2+ release channel, operating as a dual sensor of luminal pH and Ca2+. J. Biol. Chem. *285*, 35039–35046.

Raines, S.M., Rane, H.S., Bernardo, S.M., Binder, J.L., Lee, S.A., and Parra, K.J. (2013). Deletion of vacuolar proton-translocating ATPase V(o)a isoforms clarifies the role of vacuolar pH as a determinant of virulence-associated traits in Candida albicans. J. Biol. Chem. *288*, 6190–6201.

Ramirez-Montealegre, D., and Pearce, D.A. (2005). Defective lysosomal arginine transport in juvenile Batten disease. Hum. Mol. Genet. *14*, 3759–3773.

Raychowdhury, M.K., González-Perrett, S., Montalbetti, N., Timpanaro, G.A., Chasan, B., Goldmann, W.H., Stahl, S., Cooney, A., Goldin, E., and Cantiello, H.F. (2004). Molecular pathophysiology of mucolipidosis type IV: pH dysregulation of the mucolipin-1 cation channel. Hum. Mol. Genet. *13*, 617–627.

Saw, N.M., Kang, S.Y., Parsaud, L., Han, G.A., Jiang, T., Grzegorczyk, K., Surkont, M., Sun-Wada, G.H., Wada, Y., Li, L., and Sugita, S. (2011). Vacuolar H(+)-ATPase subunits Voa1 and Voa2 cooperatively regulate secretory vesicle acidification, transmitter uptake, and storage. Mol. Biol. Cell *22*, 3394–3409.

Selkoe, D.J., and Wolfe, M.S. (2007). Presenilin: running with scissors in the membrane. Cell *131*, 215–221.

Shilling, D., Müller, M., Takano, H., Mak, D.O., Abel, T., Coulter, D.A., and Foskett, J.K. (2014). Suppression of InsP3 receptor-mediated Ca2+ signaling alleviates mutant presenilin-linked familial Alzheimer's disease pathogenesis. J. Neurosci. *34*, 6910–6923.

Steiner, H., and Haass, C. (2000). Intramembrane proteolysis by presenilins. Nat. Rev. Mol. Cell Biol. *1*, 217–224.

Sun, B., Zhou, Y., Halabisky, B., Lo, I., Cho, S.H., Mueller-Steiner, S., Devidze, N., Wang, X., Grubb, A., and Gan, L. (2008). Cystatin C-cathepsin B axis regulates amyloid beta levels and associated neuronal deficits in an animal model of Alzheimer's disease. Neuron *60*, 247–257.

Torres, M., Jimenez, S., Sanchez-Varo, R., Navarro, V., Trujillo-Estrada, L., Sanchez-Mejias, E., Carmona, I., Davila, J.C., Vizuete, M., Gutierrez, A., and Vitorica, J. (2012). Defective lysosomal proteolysis and axonal transport are early pathogenic events that worsen with age leading to increased APP metabolism and synaptic Abeta in transgenic APP/PS1 hippocampus. Mol. Neurodegener. *7*, 59.

Tu, H., Nelson, O., Bezprozvanny, A., Wang, Z., Lee, S.F., Hao, Y.H., Serneels, L., De Strooper, B., Yu, G., and Bezprozvanny, I. (2006). Presenilins form ER Ca2+ leak channels, a function disrupted by familial Alzheimer's disease-linked mutations. Cell *126*, 981–993.

Walker, M.W., and Lloyd-Evans, E. (2015). A rapid method for the preparation of ultrapure, functional lysosomes using functionalized superparamagnetic iron oxide nanoparticles. Methods Cell Biol. *126*, 21–43.

Wilson, C.A., Murphy, D.D., Giasson, B.I., Zhang, B., Trojanowski, J.Q., and Lee, V.M. (2004). Degradative organelles containing mislocalized alpha-and beta-synuclein proliferate in presenilin-1 null neurons. J. Cell Biol. *165*, 335–346.

Wolfe, D.M., Lee, J.H., Kumar, A., Lee, S., Orenstein, S.J., and Nixon, R.A. (2013). Autophagy failure in Alzheimer's disease and the role of defective lysosomal acidification. Eur. J. Neurosci. *37*, 1949–1961.

Yamaguchi, S., Jha, A., Li, Q., Soyombo, A.A., Dickinson, G.D., Churamani, D., Brailoiu, E., Patel, S., and Muallem, S. (2011). Transient receptor potential mucolipin 1 (TRPML1) and two-pore channels are functionally independent organellar ion channels. J. Biol. Chem. *286*, 22934–22942.

Yang, D.S., Stavrides, P., Mohan, P.S., Kaushik, S., Kumar, A., Ohno, M., Schmidt, S.D., Wesson, D., Bandyopadhyay, U., Jiang, Y., et al. (2011). Reversal of autophagy dysfunction in the TgCRND8 mouse model of Alzheimer's disease ameliorates amyloid pathologies and memory deficits. Brain *134*, 258–277.

Zhang, F., Jin, S., Yi, F., and Li, P.L. (2009). TRP-ML1 functions as a lysosomal NAADP-sensitive Ca2+ release channel in coronary arterial myocytes. J. Cell. Mol. Med. *13* (*9B*), 3174–3185.

Zhang, X., Garbett, K., Veeraraghavalu, K., Wilburn, B., Gilmore, R., Mirnics, K., and Sisodia, S.S. (2012a). A role for presenilins in autophagy revisited: normal acidification of lysosomes in cells lacking PSEN1 and PSEN2. J. Neurosci. *32*, 8633–8648.

Zhang, X., Li, X., and Xu, H. (2012b). Phosphoinositide isoforms determine compartment-specific ion channel activity. Proc. Natl. Acad. Sci. USA *109*, 11384–11389.